

# Investigating Neuronal Network Dynamics Supporting Memory in the Human Brain



Thesis

Adrien A. Causse

New College  
University of Oxford

## Supervisors

Prof. David Dupret  
Prof. Timothy Denison

Trinity Term 2026

# **Abstract**

Abstract to write here

# Contents

<b>List of Abbreviations</b>	<b>8</b>
<b>1 Introduction</b>	<b>10</b>
1.I Theta oscillations in mammals . . . . .	10
1.II What about theta oscillations in humans? . . . . .	10
1.III Hypotheses and aims of this work . . . . .	10
<b>2 Assessing associative memory in human participants</b>	<b>11</b>
2.I Conceptual introduction . . . . .	11
2.I.1 Inference as an extension of associative memory . . . . .	11
2.I.1.a Definition of associative memory and inference . . . . .	11
2.I.1.b Conservation across species . . . . .	11
2.I.1.c Two-stages model: short-term and long-term memory .	11
2.I.1.d Rodent paradigms . . . . .	11
2.I.1.e Human paradigms . . . . .	11
2.I.2 The role of the hippocampal network in associative memory . . .	11
2.I.2.a Animal studies . . . . .	11
2.I.2.b Human lesion studies . . . . .	11
2.I.2.c Indirect recordings of brain electrical activity in humans (fMRI, MEG) . . . . .	11
2.I.2.d Direct recordings of brain electrical activity in humans .	11
2.II Investigating associative memory in humans using a social community task	12
2.II.1 Rationale and behavioural paradigm . . . . .	12
2.II.2 Variants and controls . . . . .	12
2.II.2.a Simple and complex tasks . . . . .	12

2.II.2.b	Scientific rationale for population diversity . . . . .	12
2.II.2.c	Stimulus types and controls . . . . .	12
2.II.2.d	Additional visual controls . . . . .	12
2.III	Quantifying behavioural performance . . . . .	12
2.III.1	Participant demographics . . . . .	12
2.III.2	Performance metrics . . . . .	12
2.III.2.a	Group-level performance . . . . .	12
2.III.2.b	Inter-individual variability and performance profiles . . .	12
2.III.2.c	Across-group comparisons . . . . .	12
2.III.3	Possible confounds and their resolution . . . . .	12
2.III.3.a	Demographic and cognitive contributors . . . . .	12
2.III.3.b	Standardised cognitive testing . . . . .	12
2.IV	Summary: why this behavioural context justifies a neural two-stage memory investigation . . . . .	12
<b>3</b>	<b>Neural activity in the online human hippocampus is paced by a 2-Hz rhythm</b>	<b>13</b>
3.I	Conceptual introduction . . . . .	13
3.I.1	Why search for a human analogue of rodent theta? . . . . .	13
3.I.2	Hypothesis . . . . .	13
3.I.3	Analytical overview . . . . .	13
3.II	Hippocampal 2-Hz tracks mnemonic engagement . . . . .	13
3.II.1	Prominent 2-Hz bursts structure hippocampal LFPs . . . . .	13
3.II.1.a	Recording hippocampal LFPs with depth EEG in humans	13
3.II.1.b	Hippocampal LFPs are paced by a 2-Hz oscillation . . .	15
3.II.1.c	Hippocampal 2-Hz oscillations are transient . . . . .	18
3.II.1.d	Validation of 2-Hz oscillations . . . . .	19
3.II.2	Hippocampal 2-Hz is selectively evoked in the memory task . . .	22
3.II.2.a	Hippocampal 2-Hz power increase with mnemonic engagement . . . . .	22
3.II.2.b	Hippocampal 2-Hz bursts are evoked by mnemonic cues	23
3.II.2.c	Hippocampal 2-Hz oscillations are not evoked by motor activity . . . . .	25

3.III Hippocampal neuronal activity is preferentially modulated at 2-Hz . . . . .	25
3.III.1 Hippocampal neurons are paced at 2-Hz . . . . .	25
3.III.1.a Basic firing properties of hippocampal neurons reveal 2-Hz rhythmicity . . . . .	25
3.III.1.b Hippocampal neurons prefer 2-Hz oscillations . . . . .	25
3.III.2 Hippocampal gamma oscillations are preferentially modulated at 2-Hz . . . . .	25
3.III.2.a Gamma activity correlates with spiking activity . . . . .	26
3.III.2.b Hippocampal gamma activity is preferentially coupled to 2-Hz phase . . . . .	26
3.III.2.c Holo-Hilbert amplitude modulation analysis confirms prevailing 2-Hz hippocampal modulation of gamma activity . . . . .	26
3.IV Hippocampal 2-Hz synchronizes neuronal activity across MTL regions . . . . .	26
3.IV.1 2-Hz oscillations are preferentially observed in the MTL . . . . .	26
3.IV.1.a 2-Hz power dominates in the MTL and particularly in the hippocampus . . . . .	26
3.IV.1.b Prominent 6-8Hz oscillations in the non-MTL were detected using tmEMD . . . . .	26
3.IV.1.c 2-Hz oscillations are not directly evoked by mnemonic cues outside the hippocampus . . . . .	26
3.IV.2 MTL neurons are paced at 2-Hz . . . . .	27
3.IV.2.a Basic firing properties of MTL neurons reveal 2-Hz rhythmicity . . . . .	27
3.IV.2.b MTL neurons prefer 2-Hz oscillations in the hippocampus . . . . .	27
3.IV.3 Hippocampal 2-Hz synchronizes MTL gamma oscillations . . . . .	27
<b>4 Neural activity in the offline human hippocampus</b>	<b>28</b>
4.I Conceptual introduction . . . . .	28
4.I.1 The two-stage model of memory . . . . .	28
4.I.2 Hypothesis . . . . .	28
4.I.3 Analytical overview . . . . .	28
4.II Hippocampal physiology across sleep stages . . . . .	28
4.II.1 Hippocampal 2-Hz features REM sleep but not SWS . . . . .	28
4.II.2 Hippocampal ripples feature SWS and rest sessions . . . . .	28

4.II.2.a	Detection of hippocampal ripples . . . . .	28
4.II.2.b	Basic properties of the ripples . . . . .	28
4.II.2.c	Ripples properties across sleep stages . . . . .	29
4.II.2.d	Hippocampal neurons are modulated by ripples . . . . .	29
4.II.2.e	Ripples propagate to the MTL . . . . .	29
4.III	Neuronal coactivity motifs in 2-Hz bursts reactivate in post-learning hippocampal ripples . . . . .	29
4.III.1	Measuring reactivation using neuronal coactivity motifs . . . . .	29
4.III.1.a	2-Hz bursts coactivity motifs reactivate in post-learning ripples . . . . .	29
4.III.1.b	Reactivation is relevant for behavioural performance . . . . .	29
4.III.2	Measuring reactivation using gamma coactivity motifs . . . . .	29
4.III.2.a	Gamma coactivity motifs are physiologically meaningful . . . . .	29
4.III.2.b	Gamma coactivity motifs are rigid . . . . .	29
<b>5</b>	<b>Discussion</b>	<b>30</b>
<b>A</b>	<b>Appendix: Neurophysiological recordings and analysis of oscillations</b>	<b>31</b>
A.I	Data acquisition and preprocessing . . . . .	31
A.I.1	Participants . . . . .	31
A.I.2	Electrode models . . . . .	31
A.I.3	Co-registration and anatomical verification . . . . .	31
A.I.4	Neurophysiological recordings . . . . .	31
A.I.5	Detection of IEDs . . . . .	31
A.II	Decomposing LFPs into oscillatory components . . . . .	31
A.II.1	Rationale for IMF-based decomposition . . . . .	31
A.II.2	Mask optimization and criteria . . . . .	31
A.II.3	Cycle detection and quality control . . . . .	31
A.II.4	Detection of oscillatory bursts . . . . .	31
A.III	Other spectral decompositions . . . . .	31
A.III.1	PSDs estimation (Welch) . . . . .	31
A.III.2	Aperiodic correction using spectral parameterization . . . . .	31

A.III.3	Morlet wavelet spectrogram parameters . . . . .	31
A.III.4	Stimulus-locked spectral amplitude estimation . . . . .	31
A.III.5	Detection of gamma activity . . . . .	32
A.IV	Cross-frequency analyses . . . . .	32
A.IV.1	PAC and phase randomization . . . . .	32
A.IV.2	HHSAs . . . . .	32
<b>B Appendix: Analysis of single-neuron activity</b>		<b>33</b>
B.I	Spike sorting and single-unit validation . . . . .	33
B.I.1	Automated pipeline . . . . .	33
B.I.2	Manual curation quality criteria . . . . .	33
B.I.3	Waveform classification . . . . .	33
B.II	Spike-field relationship . . . . .	33
B.II.1	PPC and phase randomization . . . . .	33
B.II.2	Spike-gamma relationship . . . . .	33
<b>C Appendix: Hippocampal ripples and reactivation</b>		<b>34</b>
C.I	Ripple detection and validation . . . . .	34
C.I.1	Initial ripple detection . . . . .	34
C.I.2	Template matching . . . . .	34
C.I.3	Final detection and quality controls . . . . .	34
C.I.4	Ripple-triggered averages . . . . .	34
C.I.5	Characterization of ripple central frequency . . . . .	34
C.II	Detection of cross-regional coactivity motifs . . . . .	34
C.II.1	Epochs selection . . . . .	34
C.II.2	Using single-neurons . . . . .	34
C.II.3	Using gamma activity . . . . .	34
C.III	Reactivation of coactivity motifs in hippocampal ripples . . . . .	34
C.III.1	GLMs . . . . .	34
C.III.2	Controls . . . . .	34
<b>D Appendix: Statistical analyses</b>		<b>35</b>

D.I	Bootstrap and permutation tests . . . . .	35
D.II	GLMs and LMEMs . . . . .	35
D.III	Cluster-based permutation . . . . .	35

# List of Abbreviations

**CAR** common-average reference

**CI** confidence interval

**depth EEG** depth electroencephalography

**ECoG** electrocorticography

**EMD** empirical mode decomposition

**ERP** event-related potential

**fMRI** functional magnetic resonance imaging

**GLM** generalized linear model

**HHSA** Holo-Hilbert Spectral Analysis

**IED** interictal epileptiform discharge

**IMF** intrinsic mode function

**ISOMAP** isometric mapping

**LFP** local field potential

**LMEM** linear mixed-effects model

**MEG** magnetoencephalography

**mEMD** masked EMD

**MTL** medial temporal lobe

**PAC** phase-amplitude coupling

**PPC** pairwise-phase consistency

**PSD** power spectral density

**REM** rapid eye movement

**SWR** sharp-wave ripple

**SWS** slow-wave sleep

**tmEMD** tailored-masked EMD

**UMAP** uniform manifold approximation and projection

# 1 Introduction

## 1.I Theta oscillations in mammals

## 1.II What about theta oscillations in humans?

Direct recording of hippocampal activity using depth electroencephalography (depth EEG). History. Methodological considerations and differences between electrode types. There is a gap in knowledge.

## 1.III Hypotheses and aims of this work

# **2 Assessing associative memory in human participants**

## **2.I Conceptual introduction**

Why behaviour matters for interpreting hippocampal physiology?

### **2.I.1 Inference as an extension of associative memory**

**2.I.1.a Definition of associative memory and inference**

**2.I.1.b Conservation across species**

**2.I.1.c Two-stages model: short-term and long-term memory**

**2.I.1.d Rodent paradigms**

**2.I.1.e Human paradigms**

### **2.I.2 The role of the hippocampal network in associative memory**

Keep in mind the framework of the thesis which differentiates short-term and long-term memory. And HPC vs MTL for human studies.

**2.I.2.a Animal studies**

**2.I.2.b Human lesion studies**

**2.I.2.c Indirect recordings of brain electrical activity in humans (fMRI, MEG)**

**2.I.2.d Direct recordings of brain electrical activity in humans**

## **2.II Investigating associative memory in humans using a social community task**

### **2.II.1 Rationale and behavioural paradigm**

#### **2.II.2 Variants and controls**

2.II.2.a Simple and complex tasks

2.II.2.b Scientific rationale for population diversity

2.II.2.c Stimulus types and controls

2.II.2.d Additional visual controls

## **2.III Quantifying behavioural performance**

### **2.III.1 Participant demographics**

### **2.III.2 Performance metrics**

2.III.2.a Group-level performance

2.III.2.b Inter-individual variability and performance profiles

2.III.2.c Across-group comparisons

### **2.III.3 Possible confounds and their resolution**

2.III.3.a Demographic and cognitive contributors

2.III.3.b Standardised cognitive testing

## **2.IV Summary: why this behavioural context justifies a neural two-stage memory investigation**

Transition to Chapter 3: behaviour => neural recordings

# 3 Neural activity in the online human hippocampus is paced by a 2-Hz rhythm

## 3.I Conceptual introduction

### 3.I.1 Why search for a human analogue of rodent theta?

Rodent theta: pacing learning, spatial navigation, and ensemble formation. Human low-frequency variability and the open question

### 3.I.2 Hypothesis

Human memory is organized by a slower “theta-like” rhythm. This rhythm should appear in active states, structure spikes and gamma, synchronize MTL regions, be modulated by mnemonic engagement.

### 3.I.3 Analytical overview

Oscillation decomposition (concept). Burst detection (concept). Spike-phase and gamma-phase coupling local and distal (concept). ERP-locked analyses. Point to appendices for methodological details

## 3.II Hippocampal 2-Hz tracks mnemonic engagement

### 3.II.1 Prominent 2-Hz bursts structure hippocampal LFPs

#### 3.II.1.a Recording hippocampal LFPs with depth EEG in humans

To characterize hippocampal network activity in humans, we recorded local field potentials (LFPs) directly from the hippocampus using depth EEG. Thirty-five participants

undergoing clinical monitoring for pharmacoresistant epilepsy in two centers (Toulouse and Paris) were included in this study. Electrode implantation followed clinical requirements only. Because the hippocampus is commonly involved in seizure networks (REF), electrodes were often implanted in the hippocampus (Fig. 3.1A). In this manuscript, we focussed on participants with at least one electrode implanted in the hippocampus. Participants were implanted with standard and hybrid depth electrodes (DIXI Medical in Toulouse or Behnke–Fried in Paris). Hybrid electrodes incorporated both macrocontacts and microelectrodes (tetrodes or microwires). For consistency across the two centers, macrocontacts were used to obtain LFPs and common average referencing was applied. Tetrodes were used to identify single-neuron activity next to the macrocontact (Fig. 3.1B) and are used from chapter 3.III.1 of this manuscript. Anatomical localization of each macrocontact was obtained by co-registering postoperative CT with preoperative MRI and mapping contacts to individual hippocampal volumes (Fig. 3.1C,D). For additional methodological details see Appendix A.I.

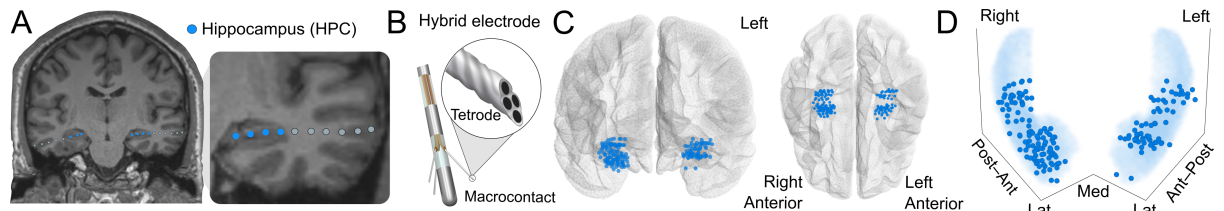


**Figure 3.1: Direct electrophysiological recordings from the human hippocampus** **(A)** T1-weighted MRI showing contact locations from two representative depth electrodes targeting the hippocampus. **(B)** Each hybrid electrode incorporated tetrodes extending from the macrocontact shaft. **(C and D)** MNI template brain and 3D projection showing hippocampal electrode contact locations across participants (axes: Post–Ant, posterior–anterior; Med–Lat, medio–lateral; Sup–Inf, superior–inferior).

We further verified the location of hippocampal contacts along the antero–posterior and medio–lateral axes of each participant’s hippocampus using their native three-dimensional segmentation (Fig. 3.2A,B). Coverage was denser in the head of the hippocampus than in the body, and virtually no contacts were located in the tail (Fig. 3.2C,D).

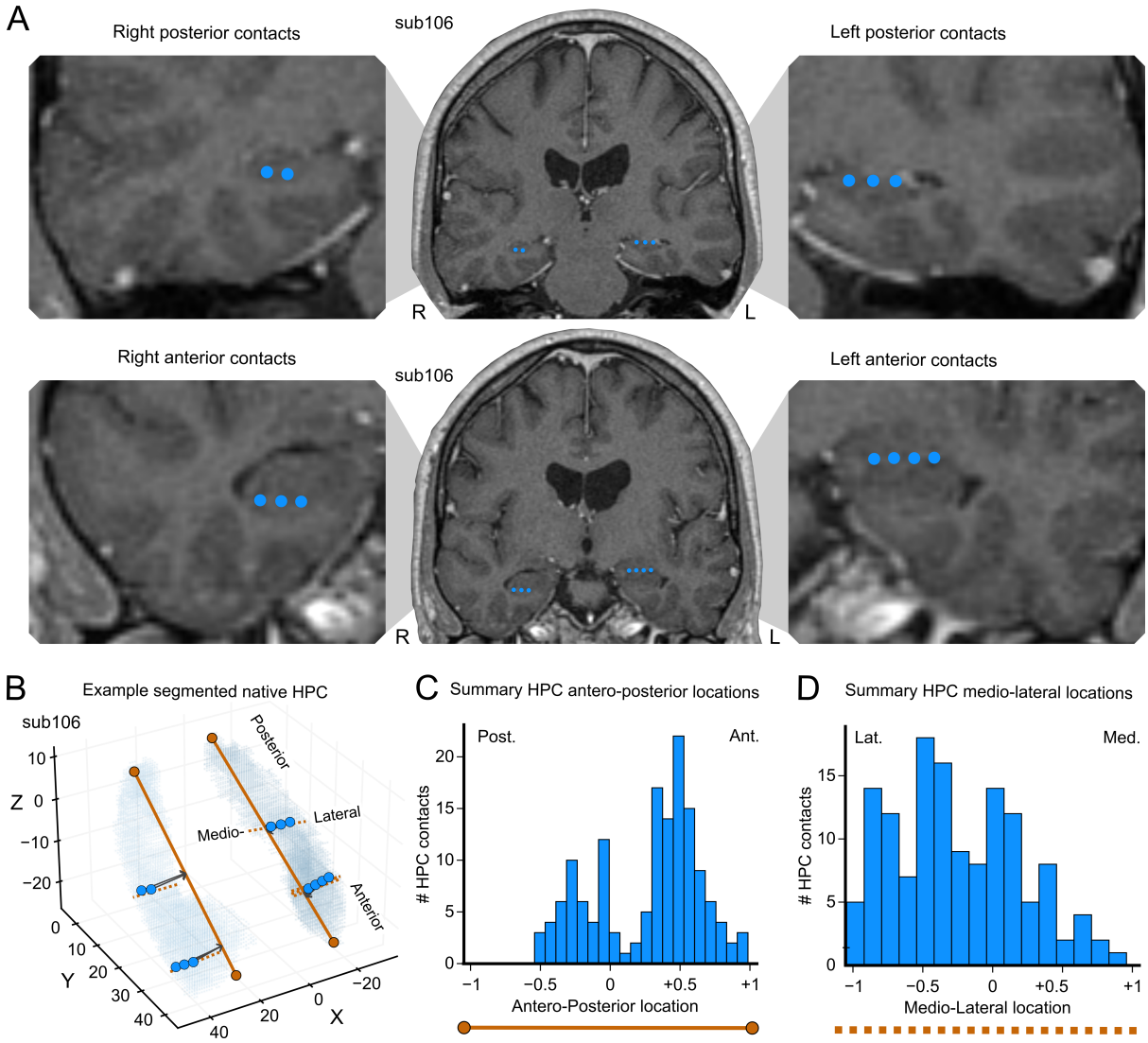


**Figure 3.2: Anatomical localization and distribution of hippocampal electrode contacts** (A) T1-weighted MRI showing posterior (top) and anterior (bottom) hippocampal electrode contacts. Insets display higher magnifications of the right and left hemispheres. (B) 3D hippocampal volumes segmented from the same subject's MRI with contact locations (blue dots) overlaid. Solid and dotted brown lines mark the detected antero-posterior and medio-lateral axes, respectively. (C and D) Distribution of hippocampal contacts along the antero-posterior (C) and medio-lateral (D) axes across all participants. Of 170 contacts, 105 were located in the right hemisphere.

### 3.II.1.b Hippocampal LFPs are paced by a 2-Hz oscillation

Analyzing brain oscillations often involves assuming that a given biological signal lies within a strict frequency range. This approach is efficient when this biological phenomenon is well established such as theta oscillations in mice (REF), but it constrains the analysis to prior knowledge. An alternative is to use unsupervised signal decomposition methods such as empirical mode decomposition (EMD). EMD decomposes LFPs into their constituent oscillatory components (referred to as intrinsic mode functions (IMFs)) without assuming fixed frequency bands (REF). However, several factors can

influence the spectral structure of LFPs across macrocontacts and subjects. As a result, the extracted IMFs may overlap in frequency (mode mixing) or may not be detected in a consistent manner across macrocontacts or participants (low consistency) (REF). These issues make it challenging to ensure that IMFs are reliably identified across subjects. To address these limitations, we used a recently introduced version of masked EMD, referred to as tmEMD (REF). This approach introduces controlled masking signals during decomposition to reduce mode mixing and to improve the separation of oscillatory components. In addition, mask parameters are optimized across subjects, which increases the consistency of the detected components at the group level. tmEMD therefore provides a more stable and interpretable decomposition of hippocampal LFPs than standard EMD, particularly in datasets with substantial inter-individual variability. Full methodological details are provided in Appendix A.I.

In participants who were awake and watching screen displays, we detected one oscillation in the human hippocampus with a peak frequency around 6 Hz (peak [80% power band (PB): 6.15 [3.75 – 8.50] Hz]. In addition, we identified two slower rhythms centered near 2 Hz [peak (80% PB): 2.38 (1.25 – 3.50) Hz] and 1 Hz [peak (80% PB): 1.08 (0.65 – 1.50) Hz] (Fig. 3.3).

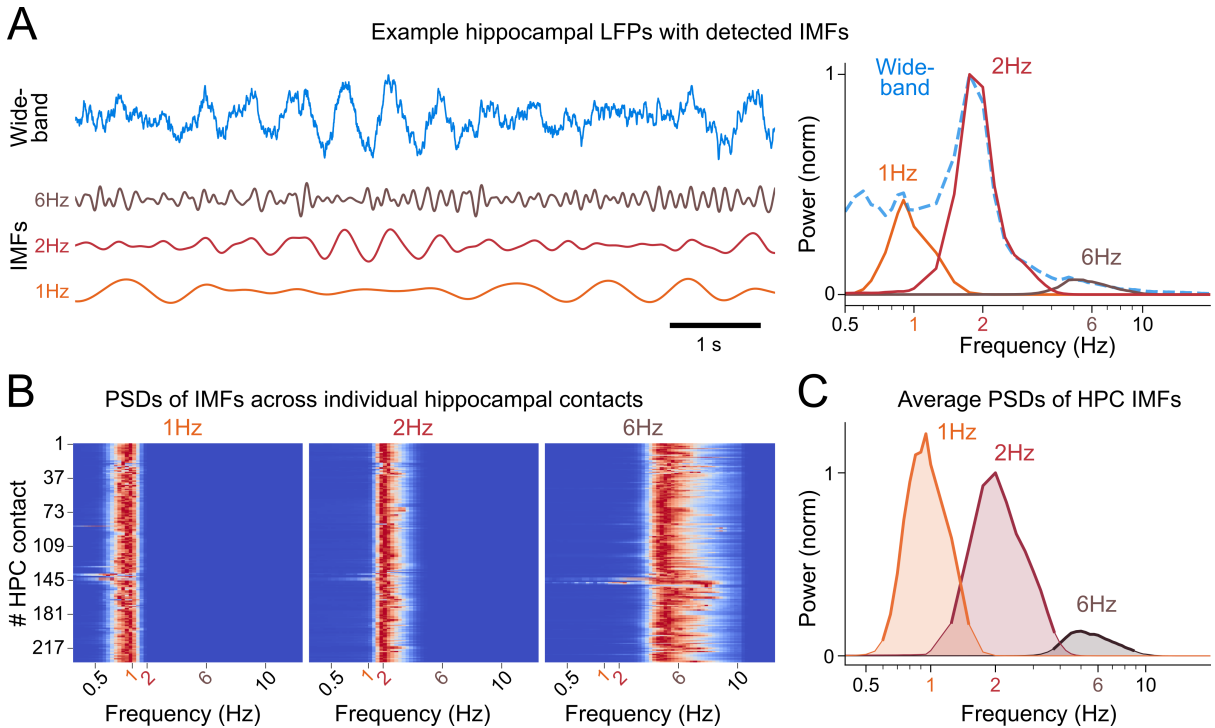


**Figure 3.3: Tailored Masked Empirical Mode Decomposition in the human hippocampus** **(A)** Left: Example hippocampal wide-band LFPs traces with IMFs. Right: Power spectral density (PSD) of the wide-band signal (dashed line) obtained from macrocontact recording and the corresponding 1-, 2-, and 6-Hz IMFs. **(B)** Heatmaps showing power distributions of 1-, 2-, and 6-Hz IMFs across all hippocampal contacts, illustrating that IMFs were consistently detected across participants. **(C)** Average power spectral densities across hippocampal contacts, normalized to the maximal 2-Hz power, showing that IMFs exhibited low mode mixing (thick lines indicate 80% power bands).

Though we were able to detect 6-Hz oscillations in the human hippocampus, the most prominent oscillation visible in the raw LFPs traces were at 2 Hz (Fig. 3.3A). These 2-Hz

oscillations were visible on both macrocontacts and tetrodes (Fig. 3.4).

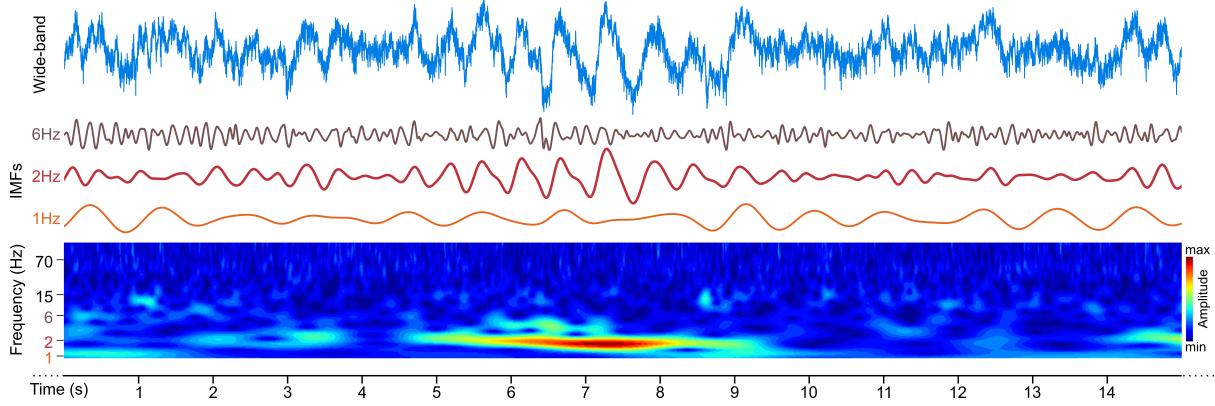


Figure 3.4: **Example hippocampal LFPs showing a 2-Hz burst** Example 15-s hippocampal tetrode recording showing a prominent 2-Hz burst. From top to bottom: wide-band LFPs trace obtained from tetrode recording, IMFs, and the corresponding wavelet spectrogram.

We confirmed this observation by applying spectral parameterization (REF; see Appendix A.III), which separates the periodic components of the power spectral density (PSDs) from the broadband, aperiodic structure of the spectrum. This procedure allowed us to quantify narrow-band oscillatory peaks independently of differences in overall spectral slope across contacts or participants. After removing the aperiodic component, the periodic residuals showed a clear prominence of the 2-Hz component in the hippocampus (Fig. 3.5A). Specifically, the corrected spectra yielded higher power at 2 Hz than at 1 Hz or 6 Hz (Fig. 3.5B), and the computed 2-Hz/6-Hz peak power ratio was consistently positive across hippocampal contacts (mean ratio [95% confidence interval (CI)]: 0.21 [0.15 – 0.27]; Fig. 3.5C). These results analysis suggest that hippocampal activity is dominated by a 2-Hz rhythm.

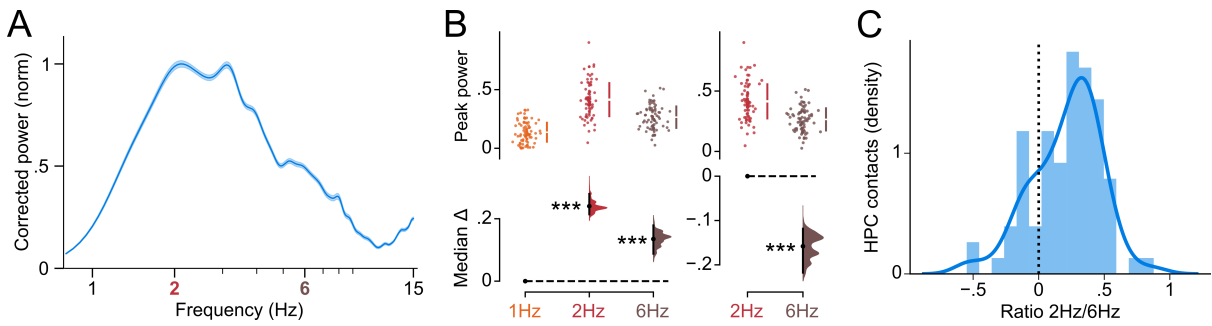
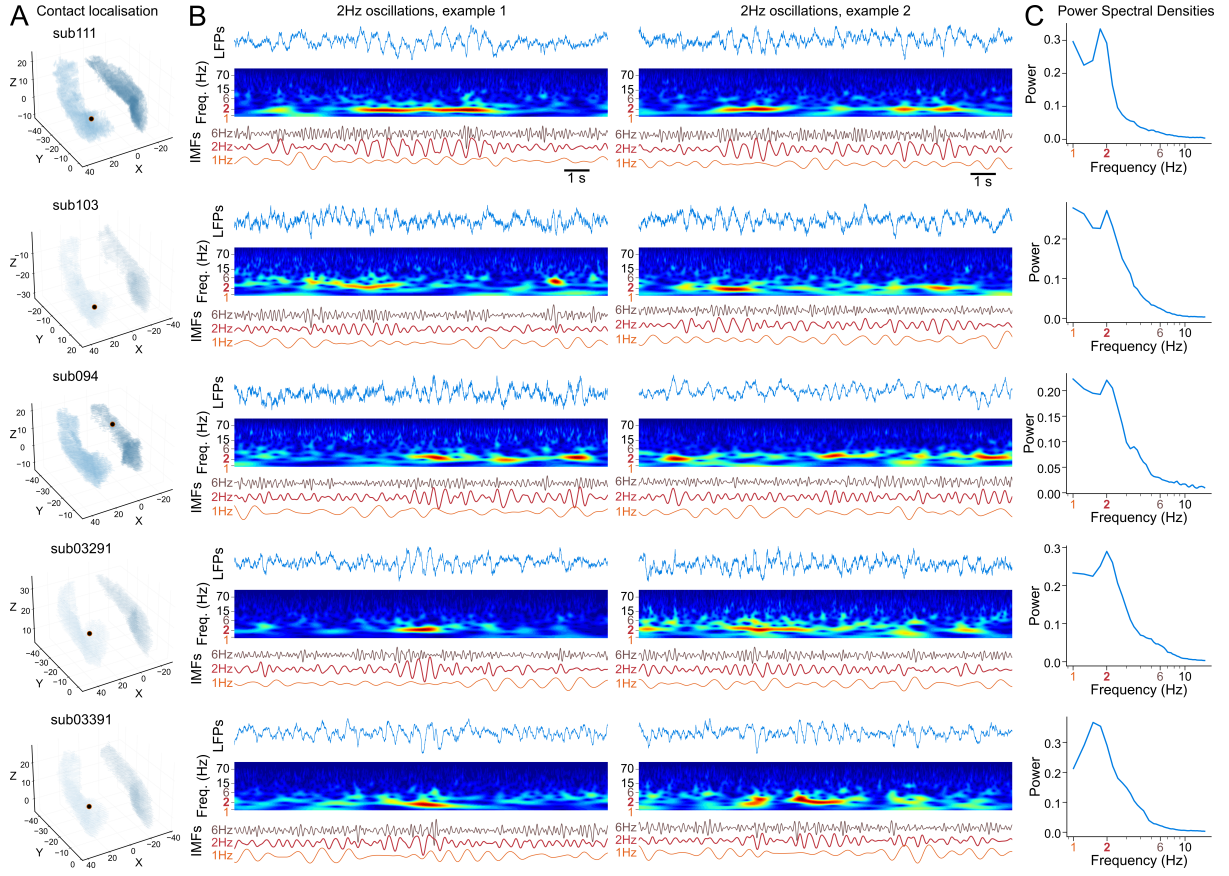


Figure 3.5: **2-Hz oscillations dominate in the human hippocampus** (A) PSDs corrected for the power law and averaged across hippocampal macrocontacts free of interictal epileptiform discharges (IEDs). Shaded areas indicate mean  $\pm$  SEM. (B) Estimation plots showing median differences between corrected 1-, 2-, and 6-Hz peak power (left), and between 2-Hz and 6-Hz peak power (right). (C) Distribution showing positive 2-Hz/6-Hz peak power ratios in hippocampal contacts. Data were analyzed by two-sided paired permutation tests; \*\*\* $P < 0.001$ .

### 3.II.1.c Hippocampal 2-Hz oscillations are transient

Hippocampal 2-Hz activity appeared as transient oscillatory bursts and was observable across subjects and along the hippocampal formation (Fig. 3.6).



**Figure 3.6: Examples of hippocampal 2-Hz bursts** (A) 3D hippocampal volumes showing electrode contact locations used in panels B and C. (B) Example 15-s hippocampal macrocontact recordings showing 2-Hz oscillations with corresponding spectrograms and (IMFs) from five participants (one row per participant). (C) PSDs averaged over the 10-min active sessions corresponding to the recordings shown in panel B. All contacts were free of IEDs (from top to bottom: 0, 0.34, 0.79, 0.33, and 0.24 discharges detected per minute).

To quantify these events, we used wavelet spectrograms to detect bursts defined as periods of increased power within the 1–4 Hz range, retaining only events lasting at least two oscillatory cycles (Fig. 3.7A). For each burst, we then measured onset, offset, and duration, expressed both in seconds and in number of cycles (Fig. 3.7B). Full methodological details are provided in Appendix A.II. Across subjects, the maximal burst duration showed substantial variability (Fig. 3.7C), consistent with the transient expression of these 2-Hz events (mean maximum number [95% confidence interval (CI)]: 19.6 [15.8 – 23.4] cycles per burst).

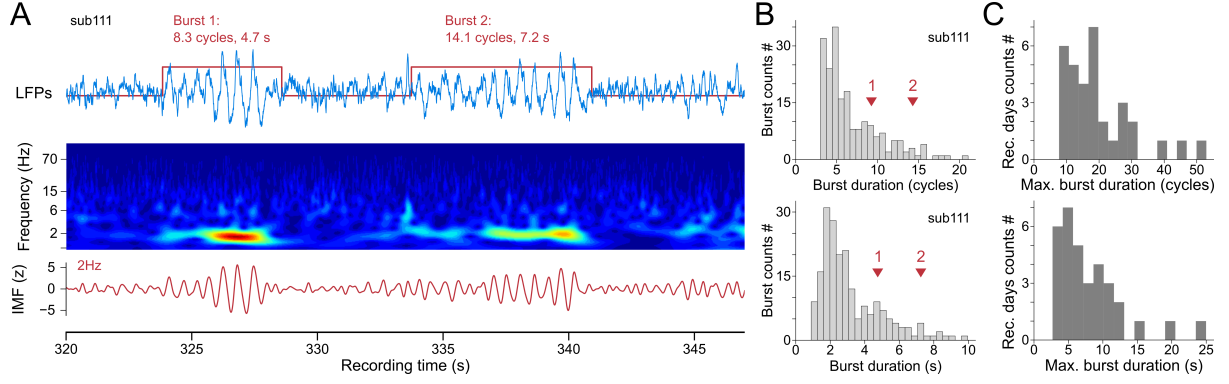


**Figure 3.7: Detection of hippocampal 2-Hz bursts** (A) Example 27-s hippocampal LFP showing 2-Hz oscillatory bursts with corresponding spectrogram and 2-Hz IMF. (B) Distributions of burst durations measured in cycles (top) and seconds (bottom) for the hippocampal macrocontact shown in panel A. A total of 174 bursts lasting at least two cycles were detected in this recall session. Arrowheads indicate the durations of the two bursts visible in panel A. (C) Distributions of maximal burst duration in cycles (top) and seconds (bottom) per recording day across participants.

### 3.II.1.d Validation of 2-Hz oscillations

#### 3.II.1.d.i Phase reversal of hippocampal 2-Hz oscillations

Hippocampal pyramidal cells are arranged in a well-defined laminar structure, which creates a consistent somato-dendritic axis that allows oscillations to be detected in LFPs (REF). When large groups of these neurons receive synchronized post-synaptic currents, the resulting transmembrane currents sum in space and form a macroscopic current dipole. This dipole generates extracellular voltage gradients that can be measured by depth electrodes as LFPs. Because this dipole is aligned across the pyramidal layer, LFPs recorded on linearly arranged contacts, i.e., spanning the somato-dendritic axis, would show a phase reversal: a same oscillatory cycle will have opposed phase on contacts located on opposite sides of the dipole. In the human hippocampus, layers are organized along the para-sagittal axis thus the dipole lies predominantly along the medio-lateral axis. The trajectories of the electrode shafts in our recordings positioned adjacent macro-contacts along this medio-lateral axis (Fig. 3.2A, left anterior contacts and Fig. 3.8A), where we observed a clear 2-Hz phase reversal (Fig. 3.8B,C). This reversal is consistent with a locally generated oscillation rather than a volume-conducted signal from a distal source (see Chapter 3.III.1 for further evidence).

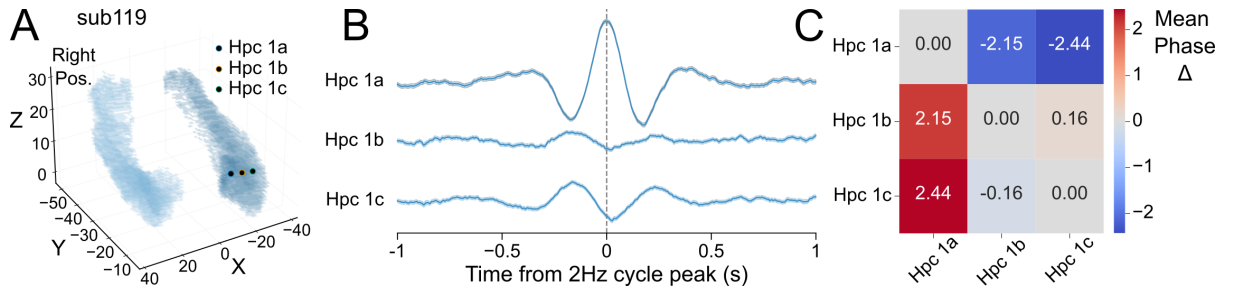


Figure 3.8: **Phase reversal of hippocampal 2-Hz oscillations** (A) 3D hippocampal volumes showing three linearly arranged recording contacts from the same electrode shaft (“Hpc 1a, 1b, and 1c”). (B) Average LFP traces aligned to hippocampal 2-Hz oscillatory peaks, showing polarity reversal across adjacent contacts. Shaded areas indicate mean  $\pm$  SEM. (C) Heatmap of average phase differences between the three contacts.

### 3.II.1.d.ii Slow-oscillation amplitude and IEDs rate

Given that these recordings were obtained from participants with drug-resistant epilepsy we next verified that hippocampal 2-Hz was not a by-product of the underlying pathology. IEDs are a common feature of epilepsy (REF) and can be reliably detected (REF janca, Fig. 3.9) from depth EEG (for further details on IEDs see Appendix A.I). IEDs rate provides an objective measure of how strongly a given tissue is affected by epileptiform activity.

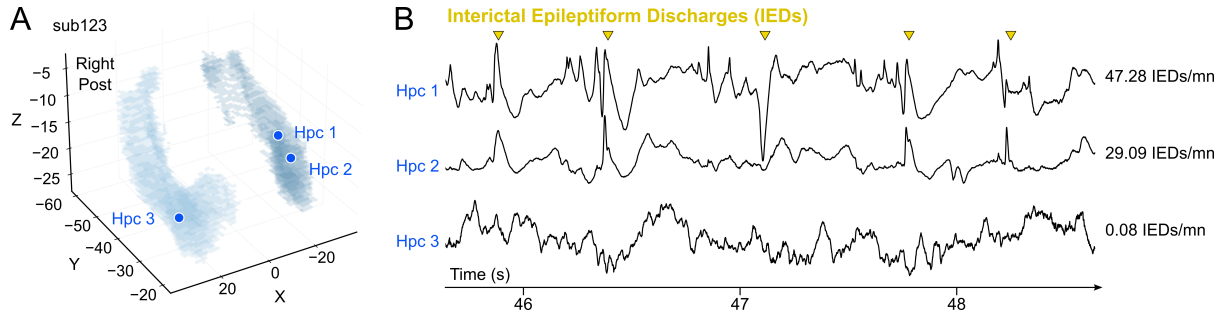


Figure 3.9: **Example of interictal epileptiform discharges** (A) 3D hippocampal volumes showing the three recording sites used in panel B. (B) Example simultaneous 3-s recording from three hippocampal contacts, with IEDs detected on “Hpc 1” (yellow arrowheads).

In these recordings, hippocampal macrocontacts with lower IEDs rates showed more prominent slow oscillations (Fig. 3.10). Consistently, 2-Hz power was negatively correlated with IEDs rate (Spearman  $r = -0.25, P < 0.001$ ), whereas 6-Hz power showed no significant relationship (Spearman  $r = 0.06, P = 0.336$ ). These results suggest that hippocampal 2-Hz rhythm is physiological and is not driven by epileptiform processes.

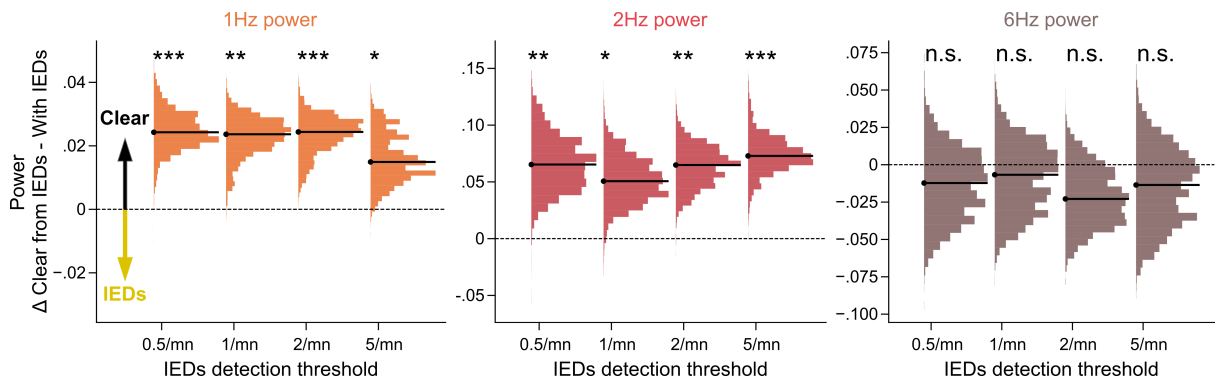


Figure 3.10: **Hippocampal slow oscillations are more prominent outside irritative zones** Estimation plots showing median differences in 1-, 2-, and 6-Hz power between hippocampal contacts free of IEDs and those containing IEDs, as a function of the IED-rate threshold (0.5, 1, 2, and 5 min<sup>-1</sup>). Data were analyzed using two-sided paired permutation tests; \*\*\*P < 0.001, \*\*P < 0.01, \*P < 0.05; n.s., not significant.

### 3.II.1.d.iii Local reference impairs detection of slow oscillations

To investigate other factors that may impact the detectability of these slower oscillations, we compared two re-referencing montages commonly used with macrocontacts (common-average reference (CAR) versus bipolar reference), and with microelectrodes (monopolar versus local reference). Bipolar and local reference involve subtracting signal from adjacent macrocontacts or tetrodes, respectively. Raw signals and in particular slow oscillations were dramatically affected by bipolar and local reference (Fig. 3.11A): they became either invisible or they showed inconsistent phase distortions. Across all hippocampal macrocontacts, bipolar/local reference impaired detectability of these slower oscillations (Fig. 3.11B–D). For this reason, all analyses in this manuscript use the CAR, which better preserves slow oscillatory components.

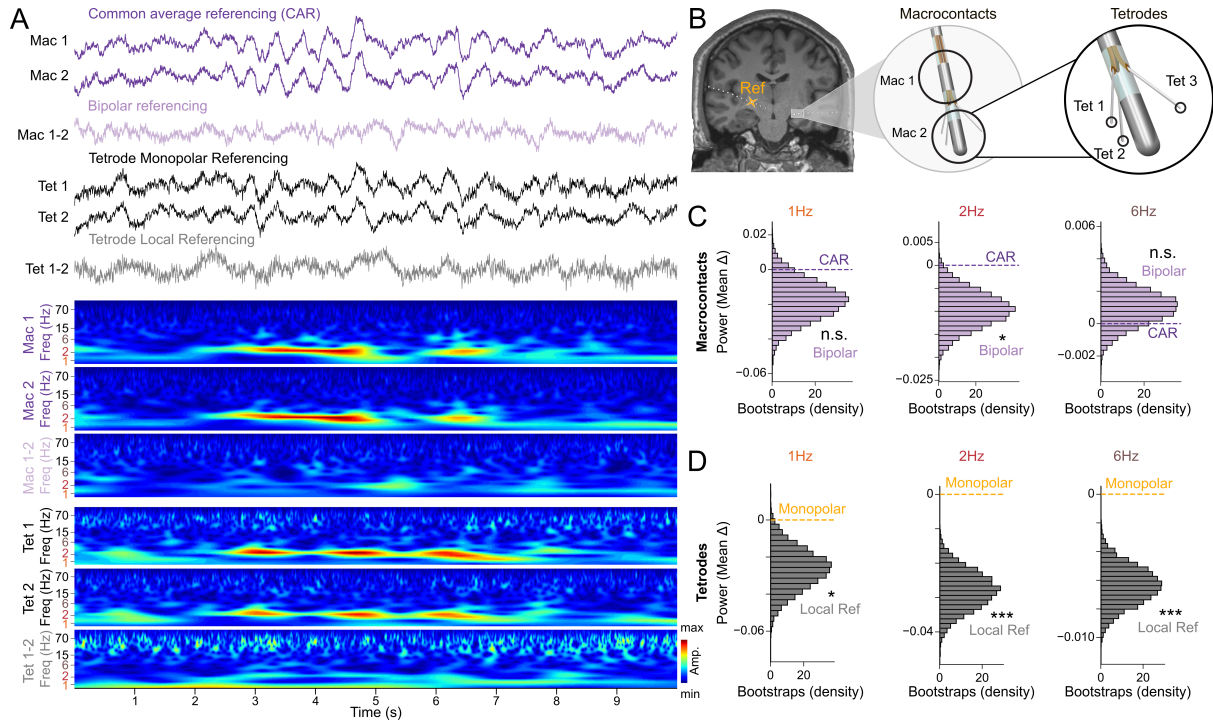


Figure 3.11: **Local reference impairs detection of slow oscillations** **(A)** Example 10-s recording from a hybrid hippocampal electrode showing macrocontact LFPs traces re-referenced using a common average (CAR, purple) or a bipolar (pink) montage, and tetrode LFPs traces before (black) and after (gray) local reference, with corresponding spectrograms. **(B)** Schematic illustrating local reference: monopolar signals were initially acquired from a distal white-matter contact and then re-referenced either to the median across all macrocontacts (common average reference, CAR) or by subtracting adjacent macrocontacts (e.g., Mac 1 – Mac 2) or tetrodes (e.g., Tet 1 – Tet 2) from the same hybrid electrode. **(C and D)** Estimation plots showing mean differences in hippocampal 1-, 2-, and 6-Hz power after applying bipolar reference to macrocontacts (relative to CAR, panel C) and local reference to tetrodes (relative to monopolar, panel D). Data were analyzed using two-sided paired permutation tests; \*\*\*P < 0.001, \*P < 0.05; n.s., not significant.

### 3.II.2 Hippocampal 2-Hz is selectively evoked in the memory task

Across participants, hippocampal LFPs revealed a prominent 2-Hz oscillation that dominated other slow rhythms and occurred in transient bursts. This rhythm showed a clear laminar phase reversal and was strongest in contacts free of IEDs, suggesting that it is a physiological rhythm. These properties indicate that hippocampal 2-Hz could be a good candidate oscillation for comparison with rodent hippocampal theta. Hippocampal theta in rodents increases during exploratory behaviour, and during memory encoding and recall (REF). In rabbits, bats and cats it is also tightly linked with sensory acquisition and is thus considered a key mechanism of active sensing (REFS). This raises two questions for the comparison with human hippocampal oscillations: does hippocampal 2-Hz also increase during memory encoding and recall, and is it similarly evoked by memory-relevant cues?

#### 3.II.2.a Hippocampal 2-Hz power increase with mnemonic engagement

To address this question we compared the changes in oscillatory power while participants were engaged in the associative memory task presented in Chapter 2. Focussing on hippocampal macrocontacts free of IEDs, we observed that 2-Hz oscillations exhibited significantly greater power during both learning and recall than during resting or viewing sessions (Fig. 3.13; learning, P < 0.001; recalling, P = 0.006; paired permutation tests compared to pre-learning rest).

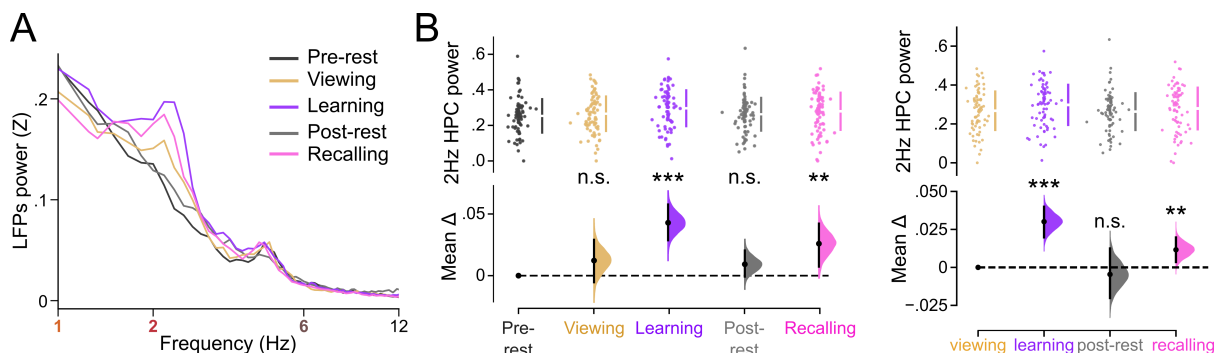


Figure 3.12: **Hippocampal 2-Hz power increases with mnemonic engagement**  
**(A)** PSDs from an example hippocampal electrode contact across task stages. **(B)** Group-level estimation plot showing mean hippocampal 2-Hz power across task stages relative to pre-learning rest (left) or viewing (right). Data were analyzed by two-sided paired permutation tests; \*\*\*P < 0.001, \*\*P < 0.01; n.s., not significant.

No comparable modulation was seen for the 1-Hz or 6-Hz bands (Fig. 3.13A). Linear mixed-effects models (LMEMs) confirmed that this enhancement was specific to 2-Hz and did not extend to adjacent frequencies (Fig. 3.13B; learning, P < 0.001; recalling, P = 0.040; Wald tests).

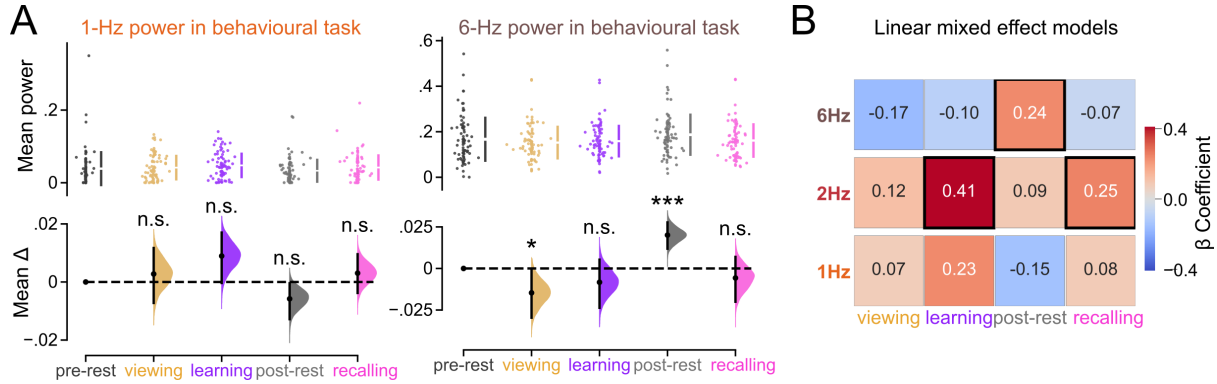


Figure 3.13: **Hippocampal oscillatory dynamics during the memory task - controls** **(A)** Group-level estimation plot showing mean hippocampal 1-Hz (left) and 6-Hz (right) power differences relative to pre-learning rest. Data were analyzed by two-sided paired permutation tests; \*\*\*P < 0.001, \*P < 0.05; n.s., not significant. **(B)** Heatmap of  $\beta$  coefficients from a LMEM predicting hippocampal 1-, 2-, or 6-Hz power as a function of task stage (pre-learning rest as the reference level), with subject treated as a random effect. Black squares indicate significant coefficients (Wald test, P < 0.05).

### 3.II.2.b Hippocampal 2-Hz bursts are evoked by mnemonic cues

While hippocampal 2-Hz activity varies with overall mnemonic engagement of the participants, it remains unclear when these oscillatory bursts occur during the task. Because visual stimuli evoke strong event-related potentials (ERPs) in the hippocampus, which manifest as broadband, non-oscillatory deflections in the LFPs, it is essential to separate these evoked responses from genuine oscillatory activity. Thus, to tease apart 2-Hz bursts from these evoked responses, we next analyze LFPs dynamics at different times relative to stimulus onset.

#### 3.II.2.b.i ERPs are modulated by mnemonic engagement

Previous work using hippocampal depth EEG has shown that the late ERPs deflection occurring at 600 ms post stimulus onset (hP600) was deeper for familiar as opposed to novel stimuli (REF Barbeau). This suggests that hippocampal ERPs are modulated by memory, which we first aimed at replicating in our behavioural task. For this, we measured average LFPs after the onset of photographs in the viewing, learning and recalling phases of the memory task (Fig. 3.14).

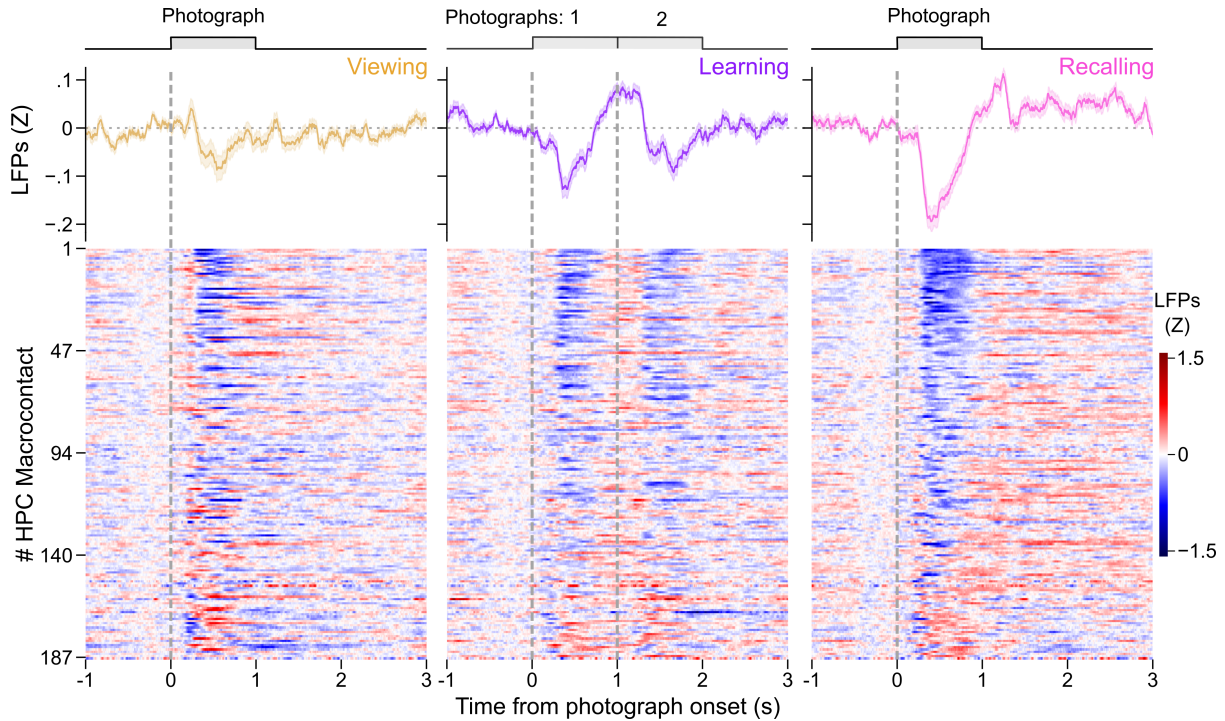


**Figure 3.14: Hippocampal ERP across task sessions** Group-level average hippocampal LFPs aligned to the onset of viewing (left), learning (middle), or recalling (right) photographic cues, with corresponding contact-level averages shown as a heatmap below. Contacts are sorted by the mean negative deflection in the recall condition for clarity. “Photograph 1” and “Photograph 2” denote the first and second paired associates presented during learning, respectively.

Consistently with earlier reports, the magnitude of the ERP deflection (hP600) was greater after the onset of learning and recalling photographs than after viewing photographs (Fig. 3.15A). In addition, ERP deflection was more pronounced for paired-associates with the best recall performance than those worst remembered, during the recall session (Fig. 3.15B). These results show that hippocampal LFP responses to visual stimuli are modulated by the mnemonic content of the photographs presented.

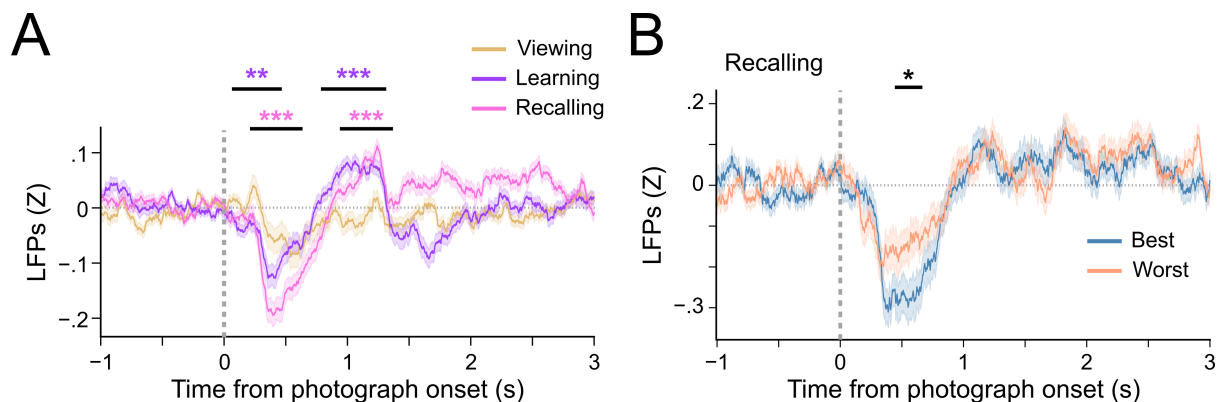


Figure 3.15: **Hippocampal ERP deflection is modulated by mnemonic engagement** (A) Group-level average hippocampal LFPss showing contrasts between viewing and learning or recall sessions. ERPs have a greater deflection after the onset of learning and recalling photographs than after viewing photographs. (B) Group-level average hippocampal LFPss showing contrasts between best and worst recalled associations during memory recall. Data were analyzed with cluster-based permutation tests; \*\*\*P < 0.001, \*\*P < 0.01, \*P < 0.05; n.s., not significant.

### 3.II.2.b.ii Evoked oscillations follow ERPs deflection

Evoked 1-, 2- and 6-Hz amplitudes relate to mnemonic engagement. Correlation between evoked ERPs deflection and 2-Hz amplitude.

### 3.II.2.c Hippocampal 2-Hz oscillations are not evoked by motor activity

Methods: Stepping sessions. Results: three example contacts (PSDs) with clear 2-Hz in learning but not during stepping. Statistics on these three subjects.

Note to myself: I could as well add a small control here, using viewing and post-viewing sessions when the participants hit the space bar (second image). Paired analysis by comparing the evoked amplitude after the first (no motor activity) and the second (motor activity) image seen in a row. It may be confounded by the short term memory effect but we don't expect this to elicit a massive 2-Hz.

## 3.III Hippocampal neuronal activity is preferentially modulated at 2-Hz

### 3.III.1 Hippocampal neurons are paced at 2-Hz

#### 3.III.1.a Basic firing properties of hippocampal neurons reveal 2-Hz rhythmicity

Methods: spike sorting and quality control. Results : firing rate distributions show that slow firing neurons constituted the biggest part of our dataset. Waveform classification: mainly broad spikes. So this looks more like pyramidal neurons. Autocorrelograms at 2-Hz. Inter-spike intervals at 500 ms.

#### 3.III.1.b Hippocampal neurons prefer 2-Hz oscillations

Methods: PPC and phase randomization. Results: cycle-triggered average of population rate to illustrate co-modulation at 2-Hz. Example spike-phase distribution reveals preference at 2-Hz. Quantification of spike-phase coupling using PPC.

### 3.III.2 Hippocampal gamma oscillations are preferentially modulated at 2-Hz

### **3.III.2.a Gamma activity correlates with spiking activity**

Methods: Detection of gamma activity (60-160 Hz). Results: Illustration of the correlation (CAR and bipolar referencing). Correlation with local VS distal gamma.

### **3.III.2.b Hippocampal gamma activity is preferentially coupled to 2-Hz phase**

Methods: PAC with the modulation index and phase randomization. Results: cycle-triggered average of gamma activity to illustrate co-modulation at 2-Hz (with spikes). Example gamma-phase distribution reveals preference at 2-Hz. Quantification of phase-amplitude coupling using PAC. Control with leave one recording day out shows that the effect is not driven by one recording day. Gamma from the anterior and posterior hippocampi prefer 2-Hz (no gradient).

### **3.III.2.c Holo-Hilbert amplitude modulation analysis confirms prevailing 2-Hz hippocampal modulation of gamma activity**

Methods: HHSA with illustration. Results: 2-Hz modulation prevails in the human hippocampus. 7-Hz oscillations dominated the mouse hippocampus.

## **3.IV Hippocampal 2-Hz synchronizes neuronal activity across MTL regions**

### **3.IV.1 2-Hz oscillations are preferentially observed in the MTL**

#### **3.IV.1.a 2-Hz power dominates in the MTL and particularly in the hippocampus**

Cycle-triggered average of LFPs show that 2-Hz oscillations propagate in the MTL. PSDs across the MTL and non-MTL contacts free of IEDs. 2-Hz vs 6-Hz power ratio.

#### **3.IV.1.b Prominent 6-8Hz oscillations in the non-MTL were detected using tmEMD**

IMF PSDs in the MTL and non-MTL with example of detected 6-8-Hz bursts in the non-MTL.

#### **3.IV.1.c 2-Hz oscillations are not directly evoked by mnemonic cues outside the hippocampus**

##### **3.IV.1.c.i ERPs deflections in MTL and non-MTL regions**

ERPs become bigger with familiarity only in the hippocampus.

##### **3.IV.1.c.ii ERPs deflection does not correlate with evoked 2-Hz bursts outside the hippocampus**

Measure evoked 1-, 2- and 6-Hz in other MTL and non-MTL regions. The measure of ERP deflections is adjusted to each region to match visual input. Correlation between

ERP deflection and evoked 1-, 2- 6-Hz oscillations.

### **3.IV.2 MTL neurons are paced at 2-Hz**

#### **3.IV.2.a Basic firing properties of MTL neurons reveal 2-Hz rhythmicity**

Results : Autocorrelograms at 2-Hz. Inter-spike intervals at 500 ms in the MTL. Example neuron in the non-MTL to show we can easily find 6-Hz rhythmicity in the non-MTL.

#### **3.IV.2.b MTL neurons prefer 2-Hz oscillations in the hippocampus**

Results: cycle-triggered average of population rate in the EC and HPC to illustrate co-modulation at 2-Hz in these two example structures. Example spike-phase distribution reveals preference at 2-Hz of EC neurons. Quantification of spike-phase coupling using PPC in the MTL. LMEMs showing that MTL gamma is better modulated at 2-Hz than non-MTL gamma.

### **3.IV.3 Hippocampal 2-Hz synchronizes MTL gamma oscillations**

Methods: distal PAC. Results: cycle-triggered average of gamma activity in the MTL. Illustration of phase-amplitude coupling across the MTL. medial temporal lobe (MTL) gamma activity is preferentially coupled to hippocampal 2-Hz phase = quantification of MTL preference for 2-Hz oscillations. Phase synchronization is higher during learning and recalling than viewing sessions.

Transition to Chapter 4: online => offline

# 4 Neural activity in the offline human hippocampus

## 4.I Conceptual introduction

### 4.I.1 The two-stage model of memory

Online (theta) → assembly formation. Offline (ripples) → assembly reactivation.

### 4.I.2 Hypothesis

Human 2-Hz bursts form the online structure for memory-relevant coactivity patterns. Offline ripples should preferentially reinstate 2-Hz-structured motifs

### 4.I.3 Analytical overview

Ripple detection and validation, coactivity motif construction. Reactivation analysis

## 4.II Hippocampal physiology across sleep stages

### 4.II.1 Hippocampal 2-Hz features REM sleep but not SWS

Methods: describe polysomnography. Example of 2-Hz bursts in REM. 2-Hz power across sleep stages. Maybe: propagation of 2-Hz oscillations in the rest of the MTL (hypothesis of the ponto-geniculocollateral oscillations PGO)?

### 4.II.2 Hippocampal ripples feature SWS and rest sessions

#### 4.II.2.a Detection of hippocampal ripples

Methods: two-step algorithm used to detect ripples. Show the templates, and the quality control used to identify reliable ripples without manual intervention.

#### 4.II.2.b Basic properties of the ripples

Show raw examples as well as ripple-triggered averages of LFPs and spectrograms. Distribution of ripple frequency centers around 70 Hz. Ripples ride on a sharp-wave. Ripples can be detected on the local tetrodes as well.

#### **4.II.2.c Ripples properties across sleep stages**

Ripple rate is higher in SWS and N1 than wake and REM. Ripples detected in rest are comparable to N1. Ripples basic properties are stable between pre- and post-learning rests.

#### **4.II.2.d Hippocampal neurons are modulated by ripples**

Trigger average (and quantification!) of the modulation of hippocampal single neurons around sharp wave ripples. Single examples and summary heatmap.

#### **4.II.2.e Ripples propagate to the MTL**

Ripple-triggered averages of the LFPs and ripple band in other regions (MTL and non-MTL). The propagation is more consistent in the MTL than the non-MTL.

### **4.III Neuronal coactivity motifs in 2-Hz bursts reactivate in post-learning hippocampal ripples**

#### **4.III.1 Measuring reactivation using neuronal coactivity motifs**

##### **4.III.1.a 2-Hz bursts coactivity motifs reactivate in post-learning ripples**

Methods: building coactivity matrices and measuring reactivation with MTL single-neurons. In-bursts vs out-of-bursts. 1-, 2- vs 6-Hz bursts (exclusion).

##### **4.III.1.b Reactivation is relevant for behavioural performance**

Learning but not viewing coactivity motifs reactivate. All controls related to learning vs viewing (firing rate, shuffled cell ID, out-of-ripples, single subjects). Best better reactivate than worst recalled associations.

#### **4.III.2 Measuring reactivation using gamma coactivity motifs**

##### **4.III.2.a Gamma coactivity motifs are physiologically meaningful**

Previous figure S18: shuffling contact IDs breaks the matrices. Intra-regional coactivity is higher than inter-regional coactivity. Correlation with 2-Hz phase amplitude coupling matrices (with illustration). Idem with ripple coactivity.

##### **4.III.2.b Gamma coactivity motifs are rigid**

All negative results on gamma coactivity, using the exact same analytical framework as with single-neurons. The aim here is to report this negative result, and echo the work done with gamma correlations in the visual field (other lab).

## 5 Discussion

Limits: what happens out of the oscillatory bursts? Noise does not exist in physiology: what information do these out-of-bursts epochs carry? These would be epochs where the firing rate is higher (aperiodic components), fractal measures are higher, but it remains unclear what is actually happening there for the network. Is it really "not" communicating with other structures? If yes, how does it communicate? What are the alternatives mechanisms to "communication through coherence"? Main challenge to study this is that the rodent hippocampus is virtually always paced by theta. Then maybe that would be the biggest inter-species difference we find: transient oscillations. Note: it could be useful to illustrate this discussion to show 6-8Hz in the temporal cortex as well.

# A Appendix: Neurophysiological recordings and analysis of oscillations

## A.I Data acquisition and preprocessing

### A.I.1 Participants

### A.I.2 Electrode models

### A.I.3 Co-registration and anatomical verification

### A.I.4 Neurophysiological recordings

### A.I.5 Detection of IEDs

## A.II Decomposing LFPs into oscillatory components

### A.II.1 Rationale for IMF-based decomposition

Here we will describe the optimization steps, final parameters of the masks used. Also Exemplify non-linearity of the signal (phase-frequency plots)

### A.II.2 Mask optimization and criteria

### A.II.3 Cycle detection and quality control

### A.II.4 Detection of oscillatory bursts

## A.III Other spectral decompositions

### A.III.1 PSDs estimation (Welch)

### A.III.2 Aperiodic correction using spectral parameterization

### A.III.3 Morlet wavelet spectrogram parameters

### A.III.4 Stimulus-locked spectral amplitude estimation

### **A.III.5 Detection of gamma activity**

## **A.IV Cross-frequency analyses**

### **A.IV.1 PAC and phase randomization**

### **A.IV.2 HHSAs**

# B Appendix: Analysis of single-neuron activity

## B.I Spike sorting and single-unit validation

### B.I.1 Automated pipeline

### B.I.2 Manual curation quality criteria

### B.I.3 Waveform classification

## B.II Spike-field relationship

### B.II.1 PPC and phase randomization

### B.II.2 Spike-gamma relationship

# C Appendix: Hippocampal ripples and reactivation

## C.I Ripple detection and validation

C.I.1 Initial ripple detection

C.I.2 Template matching

C.I.3 Final detection and quality controls

C.I.4 Ripple-triggered averages

C.I.5 Characterization of ripple central frequency

## C.II Detection of cross-regional coactivity motifs

C.II.1 Epochs selection

C.II.2 Using single-neurons

C.II.3 Using gamma activity

## C.III Reactivation of coactivity motifs in hippocampal ripples

C.III.1 GLMs

C.III.2 Controls

## D Appendix: Statistical analyses

D.I Bootstrap and permutation tests

D.II GLMs and LMEMs

D.III Cluster-based permutation